Detection and Identification of Arctic Landforms: An Assessment of Remotely Sensed Data

Kenneson G. Dean
Geophysical Institute, University of Alaska, Fairbanks, AK 99775-0800
Leslie A. Morrissey
TGS Technology, Inc., Moffett Field, CA 94035

ABSTRACT: The capabilities of remote sensing data to detect landforms on the Arctic Coastal Plain of northern Alaska were investigated. The detection and identification of thaw lakes, drained lake basins, polygonal ground patterns, pingos, eolian dunes, and drainages were assessed with both airborne and satellite-acquired data. The data included Landsat Multispectral Scanner (MSS), Thematic Mapper Simulated (TMS), NSOO1 (similar to multispectral SPOT), Seasat, and airborne radar. The remote sensing data were digitally enhanced and compared to baseline geomorphic maps derived from aerial photography.

Generally, more landforms were detected and recognized from analysis of the multispectral images than radar images because of the sensitivity of visible and infrared wavelengths to differences in vegetation and soil moisture. As expected, NSOO1 data with the highest spatial resolution, provided the basis for the most detailed photo-interpreted information and was nearly equivalent to that of high altitude aerial photography. This was the only data source that allowed detection of polygonal ground patterns. Most of the other landforms were evident on the multispectral data, but detail and recognition of these features varied. On the radar data many of the landforms were difficult to detect and/or identify due to their low surface relief. On the Seasat data differentiation of lakes was difficult due to speckle; however, draining lakes and ponds were clearly evident. Regional landforms such as paleo-shorelines from major marine transgressions could also be detected with Seasat. Airborne radar images, with low incidence angles, revealed subtle eolian dunes not evident on the multispectral sensor data. Even though most landforms could be detected on the airborne radar, many were difficult if not impossible to identify without supplemental information.

INTRODUCTION

THE ARCTIC COASTAL PLAIN of northern Alaska is located approximately 300 km north of the Arctic Circle. This region has become a focus for industrial development due to the presence of vast natural resources such as oil, gas, and coal. The Arctic is also an important region with respect to global climate and may provide critical information regarding climatic change because the effect of a global climatic warming are projected to be most severe in the boreal regions of Alaska (McBeath *et al.*, 1984.)

Remote sensing is a tool that can be utilized to monitor and analyze the arctic environment as a supplement to field observations. The detection and recognition of key landforms associated with permafrost, such as polygonal ground and thaw lakes, and the capability to monitor changes on the land surface that result from the thawing of permafrost is crucial for many arctic investigations. Image data recorded by satellite-based platforms including Landsat, SPOT, and Seasat, and by airborne sensors provide invaluable information from which arctic landforms can be studied to develop an understanding of Arctic phenomena. However, due to differences in the spatial resolution and spectral response of the various sensor systems, some are better than others for detecting or monitoring arctic surface features. The purpose of this investigation was to ascertain the potential capabilities of existing and, to an extent, proposed sensors to detect some of the pertinent landforms on the Arctic Coastal Plain of Alaska.

ARCTIC COASTAL PLAIN

The Arctic Coastal Plain of Alaska is located north of the Brooks Range and extends to the Arctic Ocean. Primary drainages include the Colville, Sagavanirktok, and Canning Rivers which are braided streams with broad floodplains. The rivers flow northward from the Brooks Range and discharge into the Arctic Ocean. Mean annual precipitation is 10 to 20 cm/yr and mean annual air temperature is approximately 10 degrees C below zero (Pewé, 1975). The plain is underlain by continuous permafrost that extends to a depth of over 400 m (Black, 1954; Pewé, 1975) and is composed of marine and fluvial deposits modified by processes that are related to the underlyuing permafrost and eolian activity. Several paleo-shorelines or strandlines are evident in the landscape due to marine transgressions and regressions (Williams *et al.*, 1977).

The presence of continuous permafrost, or perennially frozen ground, very near the surface is one of the major ecological factors that characterize the arctic tundra. It forms a barrier at the surface that prohibits water from percolating into the ground, resulting in extensive wetlands with numerous lakes and ponds (Plate 1). Almost all of the lakes are thaw lakes. These lakes and ponds, created by melting of the underlying permafrost, are continually forming, enlarging, and draining as part of the thaw lake cycle which has modified virtually all of the Arctic Coastal Plain. Many of the lakes have shallow marginal shelves that surround a central basin (Sellmann *et al.*, 1975). Often, inter-lake areas have a characteristic deranged drainage pattern with no distinct channels. Permafrost also affects vegetation by controlling drainage, by maintaining low temperatures in the root zone, and by providing an impervious substrate that restricts root growth. The land is predominantly covered by wet or moist tundra vegetation depending on local relief, with riparian vegetation zones along drainages.

The plain is relatively flat, extending from sea level to an elevation of 200 m with undulations that range from less than a metre to a few tens of metres above the surrounding terrain. On the ground, surface polygonal patterns 5 to 30 m in diameter are present and are indicative of the underlying ice deposits. The center of the polygons may be flat, high or low (Black, 1976). The melting of ground ice results in surface undulations referred to as thermokarst. Often, a thermokarst pit fills with water, enlarging by thawing the surrounding permafrost, eventually forming a pond or thaw lake. Conical-shape knolls or pingos are landforms that have a core of massive ice and pro-

PHOTOGRAMMETRIC ENGINEERING AND REMOTE SENSING,
Vol. 54, No. 3, March 1988, pp. 363–371.

0099-1112/88/5403–363$02.25/0

vide evidence for aggradation of permafrost (Mackay, 1976; Black, 1976).

Eolian processes are also active on the coastal plain, resulting in the deposition of sand and silt that forms dunes or blankets the landscape. Eolian activity was widespread during the latest Wisconsin and early Holocene time (Carter and Galloway, 1978). Vegetation has stabilized these deposits except where the groundcover has been disturbed and wind erodes the exposed sand forming blowouts. The morphology of the dunes are longitudinal, parabolic, and muti-cyclic, and are commonly the highest topographic irregularity on the plain. The topographic highs are well drained compared to the surrounding terrain and thus support different tundra plant communities than do the low-lying areas.

METHODS

The evaluation consisted of comparing landforms observed on various types of remote sensing data to baseline geomorphic maps derived from analysis of high-resolution aerial photography and limited field observations. Landforms investigated include thaw lakes, submerged margins of lakes, floodplains, polygonal ground, pingos, drainages, dunes, and escarpments or embankments. In addition, a comparative analysis was performed to detect the smallest feature, in this case lake size, by sensor type.

Two study areas were selected (Figure 1) and baseline geomorphic maps were compiled for each. The study areas, referred to as Strand and Dune, are approximately 150 square kilometres in extent and are located at 70 30′ N latitude, 156 40′ W longitude, and 70 30′ N latitude, 153 36′ W longitude, respectively. These two sites fall within eolian zones of the Arctic Coastal Plain and are representative of arctic tundra. A more detailed description can be found in the Baseline Geomorphic Analysis section.

The satellite and airborne data were digitally enhanced to optimize the detection of landforms displayed on the baseline maps and aerial photography. Preprocessing of the NS001 and TMS data involved radiometric correction for off-nadir brightening due to atmospheric effects. Enhancement techniques included contrast stretch, cubic convolution filtering, and color compositing. The resulting images were enlarged either digitally, photographically, or optically to a common base scale of approximately 1:65,000.

False-color composite images were generated for each of the multispectral images (MSS, TMS, and NS001). Analyses of the multispectral data were restricted to the visible and near-infrared bands to provide a spectrally consistent basis for comparison utilizing false color composite imagery. Analysis of the mid-infrared or thermal bands was not included in this investigation. The authors compiled a geomorphic baseline map for each of the study areas through photointerpretation of color-infrared photography, in stereo, at a common scale of 1:65,000. Conventional photo-interpretive techniques were utilized. Following compilation of the geomorphic base maps, a number of landforms evident on the CIR photography were then located on the remotely sensed airborne and satellite imagery. The photointerpreter then determined whether the feature was evident on the imagery. A detailed description of each feature, based on an analysis of the airborne and satellite imagery, was then compiled.

The nominal resolution or pixel size of the data used in this investigation was compared to the minimum size of thaw lakes that were observed on data at the approximate scale of 1:65,000. The images were examined and the smallest recognizable lakes were selected for each type of imagery. The lakes were all less than five hectares in size. These lakes were then measured and their areas calculated. Criteria for selecting the lakes were (1) pixel brightness levels were low, appropriate for water; (2) the brightness levels within each lake were relatively consistent; and (3) the presence of an observable shoreline that did not completely conform to pixel shapes.

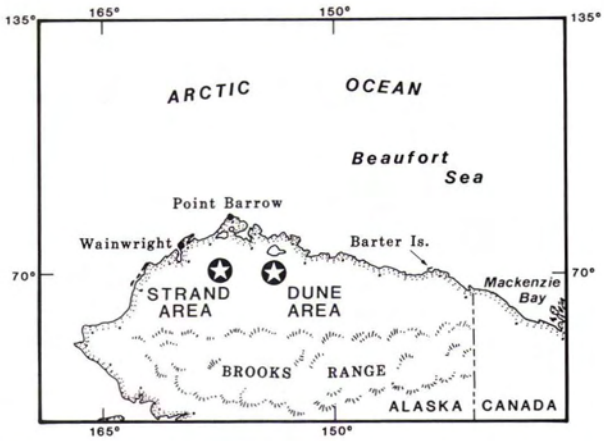

FIG. 1. Location of the Strand and Dune study areas on the Arctic Coastal Plain of northern Alaska.

AIRBORNE AND SATELLITE DATA

Landsat Multispectral Scanner (MSS), Thematic Mapper Simulator (TMS), NS001 multispectral scanner data (similar to SPOT characteristics), and Seasat and airborne radar data were used for the comparison. A summary of spectral and spatial characteristics for each type of remotely sensed data can be found in Table 1 and the imagery is shown in Figures 4 to 10.NS001 scanner data, acquired 26 August 1985 from a C130 aircraft platform, resembles SPOT data in both spectral and spatial resolution. These data were analyzed in lieu of SPOT data (which was not available) to provide an indication of the capability of high resolution satellite imagery for arctic studies. SPOT multispectral bands include 0.50 to 0.59 μm, 0.61 to 0.68 μm, and 0.79 to 0.89 μm with a 20-m spatial resolution. These closely resemble the band configuration of the NS001 scanner as shown in Table 1. The NS001 spatial resolution of 18.5 m is approximately 1.5 m better than 20-m SPOT satellite multispectral data and the band widths are within 0.03 micrometres.

NS001 data, at reduced resolution, also provided the basis for simulation of the TMS data. Spatial degradation was performed by averaging four (2-by-2 pixel window) 18.5 m pixels, thus creating a 37-m TMS pixel. Although the satellite-based TM data resolution of 30 m in the reflective bands is sightly better than the 37-m TMS data, the two were considered comparable for this investigation. NS001 bands that were utilized are direct analogs of TM bands 2 to 4, respectively, and were used without spectral modification. The TMS data were available only for the Strand study area. Landsat MSS data were recorded on 1 August 1976 and 12 July 1977 for the Dune and Strand areas. The resolution of these data is 80 m based on the size of picture elements (pixels).

Radar data from space-borne and airborne platforms were assessed in this analysis. Seasat data were recorded by a satellite-based sensor on 19 July 1978 and acquired from the Jet Propulsion Laboratory. The data are L-band synthetic aperture with a high incidence angle of 80 degrees and maximum nominal range resolution of 25 m. The Seasat data encompass the Strand study area.

The X-band airborne radar data were recorded in August, 1979 and 1980 by a U.S. Army reconnaissance aircraft and by a commercial company contracted by the U.S. Geological Survey (USGS). The Army data were acquired of the Strand study area

TABLE 1. REMOTE SENSING DATA

Sensor	Theoretical Spectral Bandwidth (μm)	Resolution
Aerial Camera RC-10	Color Infrared Film	2 m
Landsat Multispectral Scanner	0.5 - 0.6*	80 m
	0.6 - 0.7*	
	0.7 - 0.8	
	0.8 - 1.1*	
Thematic Mapper Simulator	0.45- 0.52	37 m
	0.52- 0.60*	
	0.63- 0.60*	
	0.76- 0.90*	
	1.55- 1.75	
	2.08- 2.35	
	10.4 -12.50	
NS001 Multispectral Scanner (Similar to SPOT)	0.52- 0.60*	18.5 m
	0.63- 0.69*	
	0.76- 0.90*	
Seasat Radar Synthetic Aperture	L-band (23.5 cm)	25 m
Airborne Real Aperture Radar (RAR)	X-band (3.1 cm)	30 m
Synthetic Aperture (USGS SAR)	X-band (3.1 cm)	15 m

*Channels utilized in the photointerpretation

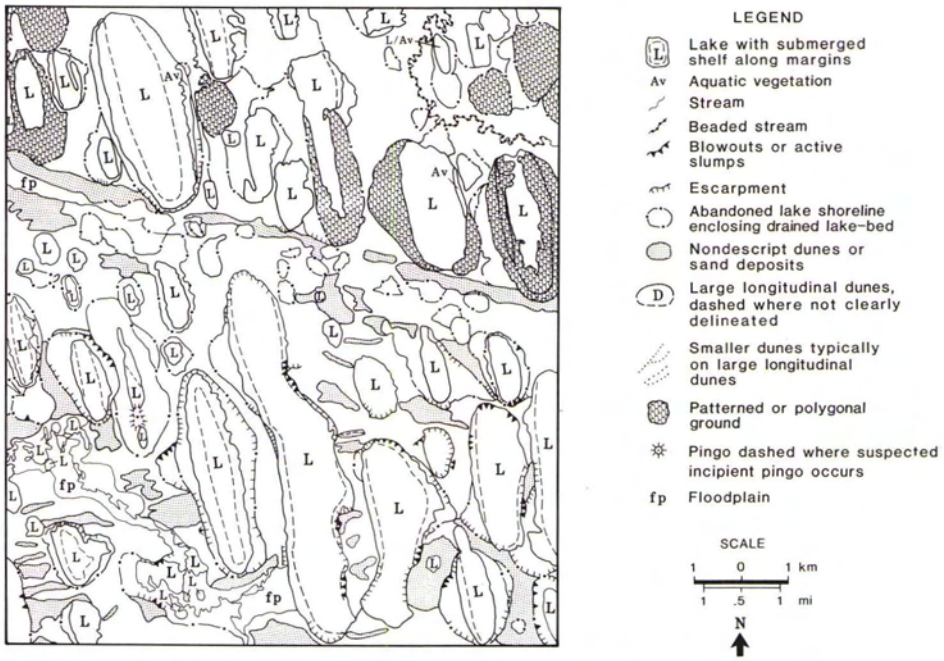

FIG. 2. Baseline geomorphic map of the Strand Study Area.

by a real aperture radar (RAR) with an incidence angle of 4 to 45 degrees and a resolution of approximately 30 m. The USGS data were acquired of the Dune study area by a synthetic aperture radar (SAR) with an incidence angle of 10 to 40 degrees and a published resolution of approximately 15 m. The airborne radar images were initially recorded optically and then were digitized so that computer-generated enhancements could be utilized.

The detection and recognition of landforms with the various remote sensing data are also distinguished in the discussion. The ability to record the presence of features by an imaging system is referred to as detectability. However, the identity or

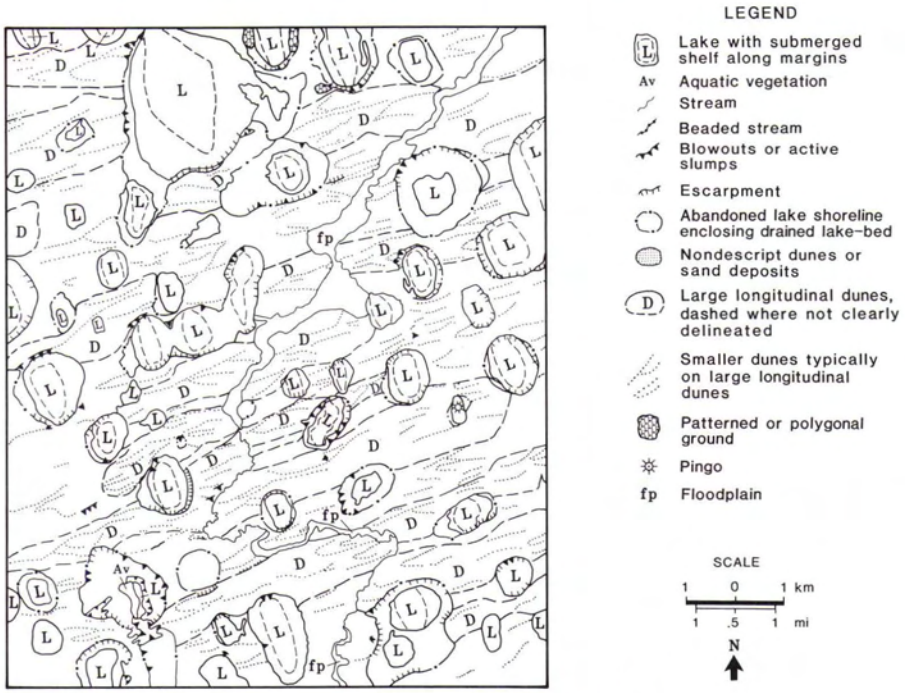

FIG. 3. Baseline geomorphic map of the Dune Study Area.

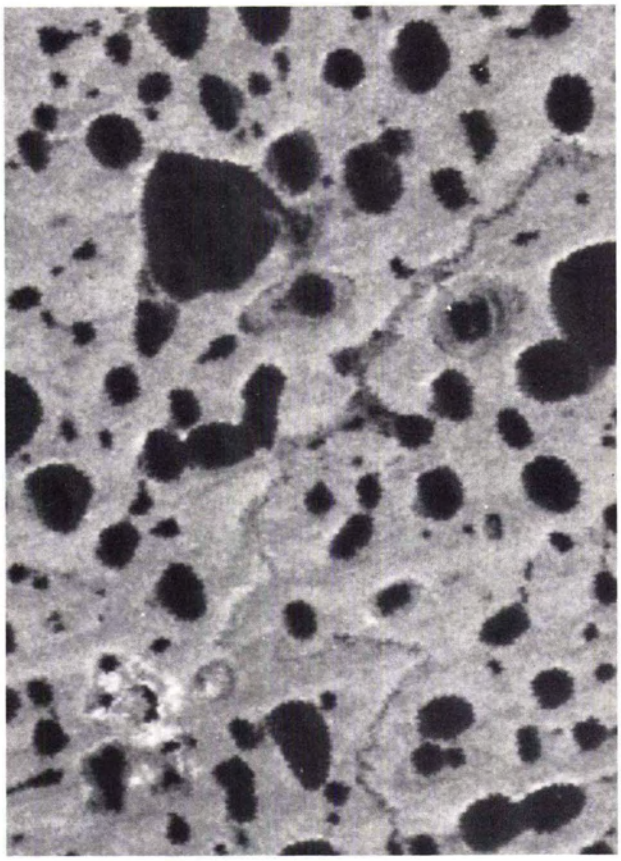

FIG. 4. Landsat MSS image of the Dune Study Area.

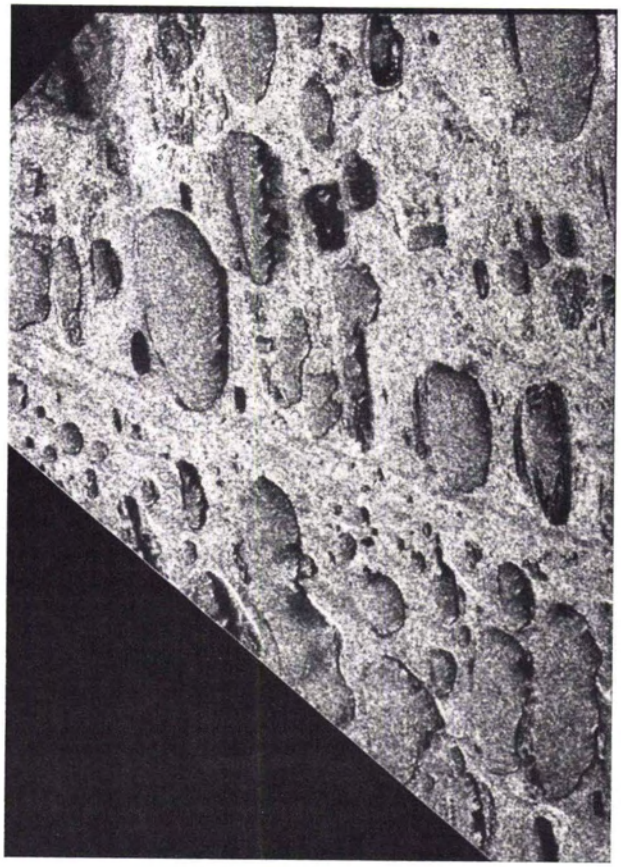

FIG. 5. Seasat image of the Strand Study Area.

recognition of the feature may still be unknown (Sabins, 1987). Usually, detectability is limited by pixel size and recognition by contrast, tone, color, shape, and texture of the feature and the investigator's experience. Often, remote sensing data will allow detection of a feature but not identification.

FIG. 6. Airborne radar image of the Strand Study Area.

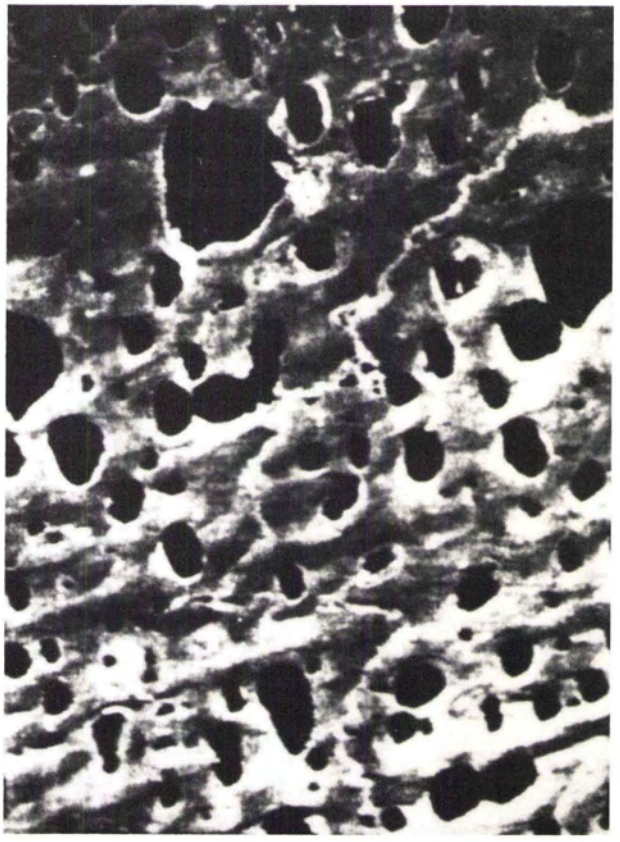

FIG. 7. Airborne USGS radar image of the Dune Study Area.

BASELINE GEOMORPHIC ANALYSIS

STRAND STUDY AREA

The Strand Area is dominated by landforms derived from processes primarily associated with permafrost (Figure 2). Thaw lakes, abandoned lake shorelines, and drained lake beds are the principal landforms that can be observed on the photography. Many of the lakes have submerged marginal shelves and a few have aquatic vegetation near shore. Slumping was observed along some shore embankments but was not mapped due to the small size of the features. Some slumping appears to be associated with blowouts.

Inter-lake areas are relatively flat with numerous ponds and few distinct drainages. Two clearly evident drainages are the Okpiksak River, which is a beaded stream, and an unnamed drainage that has developed a floodplain. The presence of oxbows, meander scars, cut banks, escarpments, and contrasting vegetation define the extent of the floodplain. Vegetation along these drainages is tall brush, mostly willow, which has a bright red signature on the photography compared to the pink signature of the surrounding tundra. The tundra encompasses both moist and wet vegetation communities with water at the surface in many areas.

Polygonal ground was observed on most of the drained lake beds, but only those patterns that are large and distinct were mapped on the CIR photography. A pingo-like structure is evident on the photographs in a southwest quadrant thaw lake. The structure has characteristics indicative of a pingo including a quasi-conical shape and a typical bright spectral signature in the infrared due to lush vegetation that develops in unsaturated substrate. However, there is very little relief as observed in the field and its surface has numerous small polygons. On the map (Figure 2) the structure is referred to as a suspected incipient pingo.

Large portions of lake shorelines have a steep to near-vertical gradient, although relief is not as great as observed in stereo-viewing. Those that are steepest, with the greatest relief, are mapped as escarpments. The steep shorelines are associated with the thawing of permafrost and the presence of eolian deposits and dunes. A series of enechelon dunes extends across the central portion of the area and coincides with a paleo-shoreline (strandline) described by Williams *et al.* (1977). South of these dunes, eolian deposits mantle the landscape (Williams, 1983) with numerous blowouts that are often associated with scarps.

Generally, north of the enechelon dunes the terrain is pockmarked with numerous ponds, small lakes, and wetlands with distinct polygonal patterns. To the south fewer lakes and ponds are evident with smaller polygons observed in areas where patterned ground occurs.

DUNE STUDY AREA

The Dune area (Figure 3) is dominated by eolian deposits primarily consisting of large longitudinal dunes. These dunes have been stabilized by low-lying tundra vegetation, with some blowouts occuring along embankments or scarps adjacent to lakes. Few if any ponds or wetlands that could be detected on the photography occur on these large dunes. On the large dunes are numerous smaller longitudinal and parabolic dunes. These small dunes appear to be sparsely vegetated with exposed sand where blowouts occur and thus are probably periodically active.

Numerous thaw lakes with abandoned shorelines and drained lake beds are present in interdunal areas. Presumably, the eolian deposits overlie these landforms throughout the area. The

number of inter-lake ponds, bogs, and areas with discernable polygonal ground are significantly less when compared to the Strand study area. Wet tundra is the dominant vegetation between the dunes. The primary stream traversing the area has developed a floodplain to the north and is incised into the landscape to the south. The stream and floodplain is bounded by eolian deposits that result in escarpments or embankments along the margins. Many subordinate streams, with distinct channels, flow between the lakes or into the primary stream. The streams often support brushy vegetation consisting mostly of willow which contrasts with the low-profile tundra vegetation on the dunes. Aquatic vegetation is present near the shore of some lakes, and submerged shelves are present along the margins of many lakes. The lake shelves appear to have morphological features or textures similar to dunes and thus may be composed of eolian deposits. These shelves are more extensive and occur in more lakes than in the Strand area.

COMPARISON OF REMOTE SENSING DATA

Remotely sensed data were compared to the baseline geomorphic maps for the two study areas to assess the utility of the various types of data to detect and identify arctic landforms. The ability to detect specific landforms is discussed for each type of remotely sensed data.

Landsat MSS Data (Strand and Dune Area)

On the MSS image of the Strand area (Plate 2) and the Dune area (Figure 4), thaw lakes larger than approximately three hectares (175 m by 175 m) are recognizable although most shorelines have a saw toothed appearance. Smaller water bodies alter pixel brightness-levels such that the presence of water can be inferred. Abandoned shorelines and drained lakes can be observed, at least for larger lakes. The pingo in the Dune study area can be discerned due to contrasting vegetation and the circular shape although they are difficult to identify. The Okpiksak and the unnamed river cannot be seen on the data, but the associated floodplain can be observed, again due to contrasting vegetation. Subordinate drainages cannot be detected.

The large dunes are evident in both areas (Plate 2 and Figure 4) due to their shape, texture, and slight difference in color compared to the surrounding terrain. The morphology and the orientation of these dunes are evident. A few of the larger blowout features can also be detected but are difficult to recognize.

Landforms that could not be detected are polygonal ground, beaded drainages, submerged lake-shelves, escarpments, and aquatic vegetation. Other features that could not be recognized are small lakes and ponds, the small dunes overlying the longitudinal dunes, nondescript eolian deposits, and most of the blowouts.

TMS Data-Simulated Landsat TM Data (Strand Area Only)

On the TMS image of the Strand area (Plate 3), thaw lakes larger than approximately one hectare (100 m by 100 m) are recognizable. Most of the lakes displayed on the aerial photography can be detected on the TMS image. Water bodies smaller than one hectare tend to conform to pixel patterns, usually do not have unique spectral response, and their shape tends to be blocky; however, their presence can be infrared. Most of the lake shorelines that have been abandoned and their associated exposed lake beds are clearly evident. The presence of submerged lake shelves was not clearly observed but subtle signatures in the water suggest that they may be detectable with appropriated digital enhancement.

The enechelon dunes and many nondescript eolian deposits south of the dune can be observed on the image. Unlike on the MSS images, subtle vertical relief associated with the dunes and escarpments can be discerned due to shadows. Lakes south of the enechelon dunes tend to be below the surrounding ground surfaces with steep embankments near shoreline. Most of the blowouts seen on the photography can also be discerned on the TMS image.

The Okpiksak and the unnamed river can easily be discerned and their floodplains are well defined. Contrasting vegetation and in some cases the presence of escarpments or cut-banks delineate the floodplains. The suspected incipient pingo is readily apparent on the data. Oxbows and meander scars were not seen, and the beaded nature of the Okpiksak River is not clearly recognizable. A few of the subordinate streams that drain or interconnect thaw lakes could not be discerned except for in a few areas. The presence of polygonal ground was not detected but its presence is suggestive in some areas by alternating patterns of dark and light tones.

NS001 Data-Similar to Multispectral SPOT Data (Strand Area Only)

Almost all of the landforms mapped from the aerial photography were detectable and recognizable on this imagery of the Strand area (Plate 4). Thaw lakes and ponds larger than 0.6 hectares (75 m by 75 m) were recognizable. Their shape and orientation are evident and shorelines are not blocky. Water bodies smaller than 0.6 hectares tend to conform to pixel patterns. Most if not all abandoned lake shorelines and drained lake beds observed on the photography were detected. The capabilities of these data to detect and delineate dunes, nondescript eolian deposits, the suspect incipient pingo, blowouts, escarpments, subordinate drainages, and floodplains were better than that of the TMS data. The beaded nature of the Okpiksak River is also clearly evident on the NS001 data, and large patterns of polygonal ground are apparent but still not as clearly defined as on the photography. For the most part, the NS001 data contains most of the geomorphic information that is displayed on the photography with the exception of polygonal ground in which only larger patterns can be observed.

Seasat Radar Data (Strand Area Only)

This Seasat image of the Strand area (Figure 5) displays recognizable lakes that are larger than approximately 2.5 hectares (160 m by 160 m). Most of the lakes have a "salt and pepper" signature (referred to as speckle) due to the roughness of the water surface caused by high velocity winds at the time of the satellite pass. The speckle signature of the lakes is similar to the surrounding terrain but darker. This signature is not unusual for inland lakes on Seasat images due to the high incidence angle of the data (personal communication, J. Ford, Jet Propulsion Laboratory). If the wind were calm and, hence, water surface less choppy, the size of recognizable lakes would probably be greater. In some areas the speckle signature of water and land is so similar that it is difficult to distinguish existing thaw lake shorelines.

For the most part, abandoned shorelines and the associated drained lake beds are not clearly discerned on the image. A few of the larger lake beds can be observed based on their slightly darker signature and often by the presence of several short, linear features aligned parallel to the long axis of the lake bed. The submerged lake shelves could not be detected, and no consistent variations in the water surface roughness associated with submerged lake shelves were observed. The Okpiksak River and floodplain could be discerned on the image but were difficult to recognize despite distinct differences in the vegetation, soil moisture, and topography compared to that of the surrounding terrain. Actively draining lakes are particularly evident on the Seasat image due to bright tones caused by aquatic wetlands

PLATE 1. Aerial photograph of the Arctic Coastal Plain exemplifying thaw lakes, drained lake basins, and polygonal ground patterns.

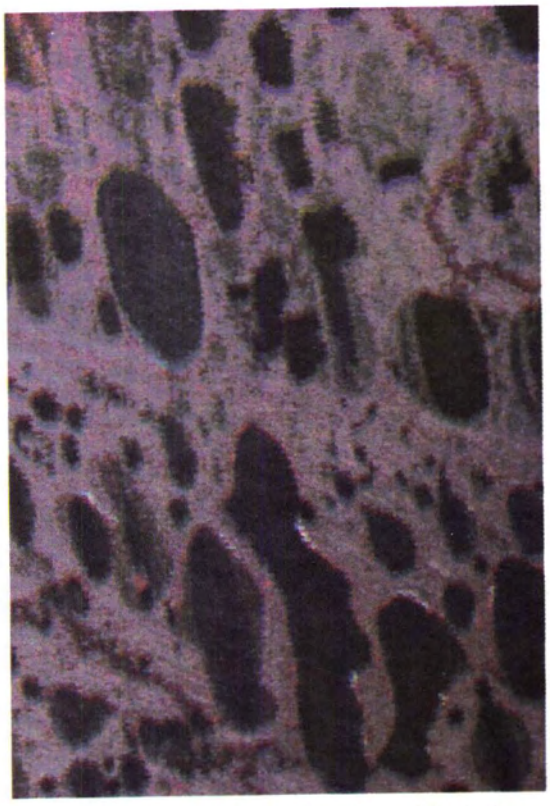

PLATE 2. Landsat MSS image of the Strand Study Area.

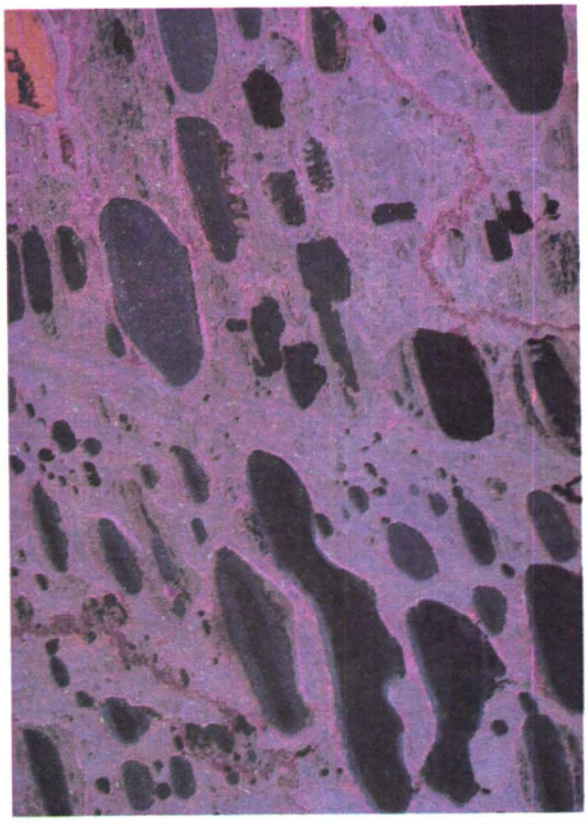

PLATE 3. Thematic Mapper Simulator (TMS) image of the Strand Study Area.

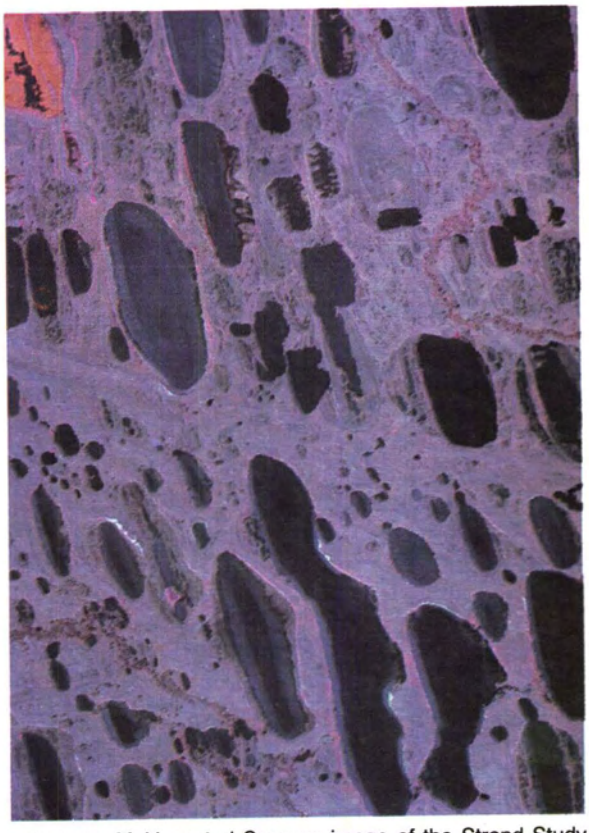

PLATE 4. NS001 Multispectral Scanner image of the Strand Study Area. The spatial resolution and spectral band intervals are similar to SPOT data.

and would be a beneficial source of information in studies of the thaw lake cycle for identifying draining lakes.

The enechelon dunes were clearly delineated but nondescript eolian deposits south of the dunes could not be seen. Many embankments or escarpments that are facing the sensor have a bright signature and, hence, can easily be detected. However, those that face away or are parallel could not be detected due to radar geometry and background noise. Other landforms that could not be seen on the Seasat image include polygonal ground, blowouts, and the beaded nature of the Okpiksak River.

The attributes of radar to detect landforms that result in surface undulations are well known (Sabins, 1987; Siegal and Gillespie, 1980). However, the subtle relief on the Arctic Coastal Plain and the high incidence angle of Seasat radar could not, for the most part, detect the landforms. A lower radar incidence-angle would significantly improve the detection of many of the landforms as evident in the airborne data.

Airborne Radar Data (Strand Area Only)

Thaw lakes were detected and recognized with the airborne RAR data of the Strand area although those lakes smaller than 1.5 hectares can be confused with topographic shadows (Figure 6). Abandoned shorelines and drained lake beds can, for the most part, be distinguished and recognized. Low-lying, flat areas, such as drained lake beds, have a bright signature and smooth texture compared to the surrounding terrain. The stream channel of the Okpiksak and the unnamed river cannot be seen. However, their floodplains can be discerned, although some segments are barely recognizable, but not the stream channel. Typically, the floodplain has a signature similar to that of drained lake beds. Some inter-lake drainages can also be detected and are recognizable. The suspected incipient pingo was detected but was not recognizable without supplemental data.

The longitudinal dunes in the Strand area are clearly delineated due to abrupt changes in the overall terrain textures north and south of the feature and due to its linear shape. South of the dune the terrain consists of numerous knolls composed of eolian deposits (nondescript dunes) that have a dark signature compared to the bright signature of the flat low-lying areas. North of the dune the image reveals fewer knolls with more low-lying areas. Embankments and escarpments are also evident, especially when they are adjacent to low-lying areas where contrast is the greatest.

Landforms that could not be detected on the airborne radar data include polygonal ground patterns, beaded streams, blowouts, submerged lake-shelves, and small water bodies.

USGS Radar Data (Dune Area Only)

Thaw lakes in the Dune area could be detected and recognized on the image (Figure 7) although smaller ones (5 hectares or less) do not have a signature that can be distinguished from the surrounding terrain. Some drained lake beds and abandoned shorelines can be seen but are not always recognizable. Stream channels were not evident but floodplains were observed. In some areas the stream valley is lost to view where it is narrow and wends between dunes. Subordinate drainages, embankments, and escarpments could also be distinguished.

The large longitudinal dunes are the most striking landform on the image, especially in the mid to far range where the incidence angle is the lowest (20 to 40 degrees). The smaller dunes on the flanks and crests of the large longitudinal dunes could not be seen on the image. Interestingly, the large dunes were not observed during the initial analysis of the aerial photography. They appeared to be nondescript eolian deposits. The radar image revealed the shape of these landforms, and subsequent analysis indentified them as longitudinal dunes. The side-slopes of these dunes typically have a gentle gradient (3 to 6 degrees), except where lakes have breached their flanks, and are usually less than 30 m above the surrounding terrain.

Landforms that could not be detected and recognized on the airborne SAR image include small dunes that overlie the large longitudinal dunes, blowouts, submerged lake-shelves, stream channels, small water bodies, and polygonal ground. Pingos could be detected but were not recognizable without supplemental data.

DISCUSSION

Landforms on the Arctic Coastal Plain of Alaska are typically small features with relatively low relief, and are primarily related to permafrost, eolian, and fluvial processes. These landforms are clearly evident on the high-altitude aerial photography and can be detected with satellite and airborne image data to varying degrees (Table 2).

Multispectral data were significantly better than the radar data for the detection and recognition of these landforms. As might be expected, the highest resolution produced the best results, that is, the NS001 multispectral data. Most of the landforms detected and recognized on aerial photography were observed on the NS001 data, including large polygonal ground patterns and beaded streams. Polygonal ground was the most difficult landform to distinguish due to its similarity with the geometry of picture elements. Large polygonal ground patterns could be seen on the NS001 data. Blowouts and escarpments or embankments were discerned on TMS and NS001 data. Submerged lake shelves are distinct on the aerial photography but were only marginally detectable (if at all) on scanner data. Most of the other landforms that were investigated are identifiable on the multispectral data but the detail is variable depending upon spatial resolution.

Table 2. Landform Detection Capabilities of Sensor Data

	DATA SOURCE					
	MULTISPECTRAL SCANNER DATA				RADAR DATA	
Landform	MSS	TMS	NS001	Seasat	RAR	USGS SAR
Abandoned Shoreline	X	X	X	M	X	X
Beaded Drainage	N	M	X	N	N	NP
Blowout	M	X	X	N	N	N
Drained/Draining Lake Bed	X	X	X	X	X	X
Dune	X	X	X	X	X	X
Escrarpment or Embankment	N	X	X	M	X	X
Floodplain	X	X	X	M	X	X
Pingo	M	X[1]	X[1]	NP	NP	M
Polygonal Ground	N	N	X	N	N	NP
Stream Channel	X	X	X	M	N	N
Stream Valley	X	X	X	M	X	X
Submerged Lake Shelf	N	M	M	N	N	N
Subordinate Drainage	N	M	X	N	M	X
Thaw Lake	X	X	X	M	X	X
Minimum size lake (hectares)	3.0	1.0	0.6	2.5		

X – detectable and recognizable

X[1] – Landform not present in the study area; however, because they can be observed on the low resolution multispectral data, it is expected that they will be detectable.

M – marginally detectable

N – not detected

NP – not present for analysis

The radar data with low incidence angles detected most of the larger landforms such as thaw lakes, drained lake beds, and large dunes (Table 2). Small landforms, such as pingos, could be detected but could not be distinguished from other surface-relief features in the surrounding terrain. Landforms with distinct surface-relief patterns can be identified but those without look like any other knoll or depression. Areas with distinct vegetative differences were not detected but flat low-lying areas that typically have high moisture were observed.

The Seasat data with its high incidence angle and image speckle was marginally capable of detecting larger thaw lakes, drained lake beds, and dunes. Several of these features had signatures similar to the surrounding terrain and, hence, boundaries could not always be delineated. Areas with distinct vegetation patterns on flat, low-lying ground could not be differentiated. Aquatic wetlands with standing water were clearly evident and differentiated from other wetlands. A few escarpments or embankments, that appear to be significant with regards to more regional analyses, were distinct. However, the more localized landforms evaluated on this project were marginally recognizable on the Seasat data for the most part.

Generally, radar data with low incidence angles revealed numerous, subtle surface undulations but these undulations can be difficult to associate with a landform. The multispectral data revealed differences in vegetation types and in ground-surface moisture, which appear to be diagnostic conditions necessary for the recognition of landforms on the coastal plain, but provided little information regarding surface relief.

Recognizable thaw lakes had to be approximately three times larger than the resolution of the multispectral data and, on the Seasat image, six times larger than the resolution of the data. The minimum area of recognizable thaw lakes for multispectral data on the Artic Coastal Plain are: MSS, 3 hectares (5 pixels); TMS, 1 hectare (7 pixels); and NS001, 0.6 hectare (18 pixels). As the resolution increases (pixels are smaller), the area of recognizable lakes decreases but the number of pixels within the water bodies increases.

The nominal resolution of the Seasat data is relatively high (25 m) but the minimal area of a recognizable lake is 2.5 hectares (40 pixels). That is, approximately six times the resolution of the data. This is considerably larger than would be expected from multispectral data of comparable resolution. The airborne SAR and RAR data were not analyzed in this context even though minimum area of recognizable thaw lakes were measured. The airborne data were film-based but were digitized in the laboratory. Thus, a recognition analysis of these data would be more a function of the scanning digitizer element size that was selected than the resolution of the imagery.

CONCLUSIONS

An assessment of satellite and aircraft data, including multispectral scanner data and radar data, was undertaken to investigate the capability of these data to detect and identify arctic landforms. To a large degree, differentiation of landforms reflect differences in vegetation communities, which are more easily detected on the multispectral scanner data than on the radar data. On the Arctic Coastal Plain, subtle differences in relief result in dramatic changes in the vegetation community and soil moisture regime. For example, pingos are elevated and better drained than the surrounding area, resulting in a bright signature in the near infrared that conforms to the shape of the pingo, thus delineating this feature. As a result, the multispectral data are better for detection of many arctic landforms because they are more sensitive to differences in vegetation and ground moisture regimes than the radar data. The timing of data acquisition to take advantage of surface conditions or a temporal analysis could further improve the analysis of landforms or surface processes. This is easier to accomplish with the satellite data because they are routinely acquired.

The low incidence-angle airborne radar detected the subtle terrain undulations throughout the study areas that were not detected by the multispectral data and in some cases the aerial photography. However, unless a landform had a very distinct relief-shape, such as longitudinal dunes, it could not be differentiated from other knolls or depressions. A combination of multispectral and radar data with a low incidence-angle would provide the optimum information on the Arctic Coastal Plain.

The most difficult landform to discern was polygonal ground in which only large patterns were observed on the NS001 data. Difficulties arise due to the similarity between the resulting natural polygons and that of picture elements on the image. On the TMS data the resolution is only slightly greater than the largest polygon, making them difficult to detect. The higher resolution of NS001 data is less than that of the largest polygons and, hence, the larger ones can be detected. Polygonal ground could not be detected on any of the radar data that was evaluated.

ACKNOWLEDGMENTS

The authors wish to thank Dr. Jack Mellor, Bureau of Land Management, for use of the airborne radar data, Mr. Thomas George for review of the manuscript, and Dr. John Ford, Jet Propulsion Laboratory, for providing digital Seasat data. This research was supported by the NASA Terrestrial Ecosystem Program.

REFERENCES

Black, R.F., 1954. Permafrost — A Review, *Geol. Soc. of Am. Bull.* V. 65, pp. 839-856.

———, 1976. Features Indicative of Permafrost, *Annual Review of Earth and Planetary Sciences*, V. 4, Annual Reviews Inc., Palo Alto, California, pp. 75-94.

Carter, L.D., and J.P. Galloway, 1978. Southward-progressing Stabilization of Holocene Eolian Sand on the Western Arctic Coastal Plain, *U.S. Geological Survey Alaska Accomplishments during 1978*, Circular 804-B, pp. B-37 and B-38.

Hall, D.K., 1982. A Review of the Utility of Remote Sensing in Alaskan Permafrost Studies, *Inst. of Elect. and Electronic Eng.*, pp. 390-394.

Mackay, J.R., 1973. The Growth of Pingos, Western Arctic Canada, *Can. Jour. Earth Sci.* V. 10, pp 979-1004.

McBeath, J.H., G. Weller, G.P. Juday, J.E. Osterkamp, and R.A. Nevé, 1984. The Potential Effects of Carbon Dioxide-induced Climatic Changes in Alaska: Conclusions and Recommendations, *The Potential Effects of Carbon Dioxide-induced Climatic Changes in Alaska*, (J. McBeath, G.P. Juday, G. Weller, M. Murray and J.V. Drew eds.), School of Agriculture and Land Resources Management, University of Alaska, Fairbanks, Misc. Publ. 83-1, pp. 193-198.

Pewé, J.L., 1975. *Quaternary Geology of Alaska*, U.S. Geological Survey Prof. Paper 835, 139 pp. and maps.

Sabins, F.F., 1987. *Remote Sensing Principles and Interpretation*, 2nd Edition, W.H. Freeman and Comp., San Francisco, California, p. 11.

Siegal, B.S., and A.R. Gillespie (ed.), 1980. *Remote Sensing in Geology*, Wiley, New York, 702 pp.

Williams, J.R., 1983. *Engineering geologic maps of northern Alaska, Meade River Quadrangle*, U.S. Geological Survey Open-File report 83-294, 29 pp., and one map.

Williams, J.R., W.E. Yeend, L.D. Carter, and T.H. Hamilton, 1977. *Preliminary surficial deposits map of National Petroleum Reserve Alaska*, U.S. Geological Survey Open-File report 77-868, one map and one legend.